



Structural transition in sputter-deposited amorphous germanium films by aging at ambient temperature

著者	Okugawa M., Nakamura R., Ishimaru M., Watanabe K., Yasuda H.
journal or publication title	Journal of Applied Physics
volume	119
number	21
year	2016-06-07
権利	(C) 2016 AIP Publishing LLC. This article may be downloaded for personal use only. Any other use requires prior permission of the author and AIP Publishing. The following article may be found at http://scitation.aip.org/content/aip/journal/jap/http://scitation.aip.org/content/aip/journal/jap/101/7/10.1063/1.4953234 The full-text file will be made open to the public on 7 June 2017 in accordance with publisher's 'Terms and Conditions for Self-Archiving'.
URL	http://hdl.handle.net/10466/15024

doi: 10.1063/1.4953234

Structural transition in sputter-deposited amorphous germanium films by aging at ambient temperature

M. Okugawa, R. Nakamura, M. Ishimaru, K. Watanabe, H. Yasuda, and H. Numakura

Citation: [Journal of Applied Physics](#) **119**, 214309 (2016); doi: 10.1063/1.4953234

View online: <http://dx.doi.org/10.1063/1.4953234>

View Table of Contents: <http://scitation.aip.org/content/aip/journal/jap/119/21?ver=pdfcov>

Published by the [AIP Publishing](#)

Articles you may be interested in

[Thermal conductivity of sputtered amorphous Ge films](#)

[AIP Advances](#) **4**, 027126 (2014); 10.1063/1.4867122

[Nanoporosity induced by ion implantation in deposited amorphous Ge thin films](#)

[J. Appl. Phys.](#) **111**, 113515 (2012); 10.1063/1.4725427

[Low-temperature solid-phase crystallization of amorphous silicon thin films deposited by rf magnetron sputtering with substrate bias](#)

[Appl. Phys. Lett.](#) **89**, 022104 (2006); 10.1063/1.2219136

[Transition from amorphous to crystalline beta phase in co-sputtered Fe Si 2 films as a function of temperature](#)

[J. Appl. Phys.](#) **98**, 123506 (2005); 10.1063/1.2148629

[Low-temperature Al-induced crystallization of amorphous Ge](#)

[J. Appl. Phys.](#) **97**, 094914 (2005); 10.1063/1.1889227

A promotional banner for AIP Applied Physics Reviews. On the left is a small image of a journal cover titled 'AIP Applied Physics Reviews' featuring a diagram of a layered structure. The main background is dark blue with a bright light source on the right. The text 'NEW Special Topic Sections' is prominently displayed in white. Below this, it says 'NOW ONLINE' in yellow, followed by 'Lithium Niobate Properties and Applications: Reviews of Emerging Trends' in white. The AIP Applied Physics Reviews logo is in the bottom right corner.

NEW Special Topic Sections

NOW ONLINE
Lithium Niobate Properties and Applications:
Reviews of Emerging Trends

AIP Applied Physics
Reviews

Structural transition in sputter-deposited amorphous germanium films by aging at ambient temperature

M. Okugawa,¹ R. Nakamura,^{1,a)} M. Ishimaru,² K. Watanabe,² H. Yasuda,³
 and H. Numakura¹

¹Department of Materials Science, Graduate School of Engineering, Osaka Prefecture University,
 Gakuen-cho 1-1, Naka-ku, Sakai 599-8531, Japan

²Department of Materials Science and Engineering, Kyushu Institute of Technology, Tobata, Kitakyushu,
 Fukuoka 804-8550, Japan

³Research Center for Ultra-High Voltage Electron Microscopy, Osaka University, Mihogaoka 7-1,
 Ibaraki, Osaka 567-0047, Japan

(Received 13 April 2016; accepted 23 May 2016; published online 6 June 2016)

The structure of amorphous Ge (a-Ge) films prepared by sputter-deposition and the effects of aging at ambient temperature and pressure were studied by pair-distribution-function (PDF) analysis from electron scattering and molecular dynamics simulations. The PDFs of the as-deposited and aged samples for 3–13 months showed that the major peaks for Ge-Ge bonds decrease in intensity and broaden with aging for up to 7 months. In the PDFs of a-Ge of molecular dynamics simulation obtained by quenching liquid at different rates, the major peak intensities of a slowly cooled model are higher than those of a rapidly cooled model. Analyses on short- and medium-range configurations show that the slowly cooled model includes a certain amount of medium-range ordered (MRO) clusters, while the rapidly cooled model includes liquid-like configurations rather than MRO clusters. The similarity between experimental and computational PDFs implies that as-deposited films are similar in structure to the slowly cooled model, whereas the fully aged films are similar to the rapidly cooled model. It is assumed that as they undergo room-temperature aging, the MRO clusters disintegrate and transform into liquid-like regions in the same matrix. This transition in local configurations is discussed in terms of instability and the non-equilibrium of nanoclusters produced by a vapor-deposition process. *Published by AIP Publishing.*

[<http://dx.doi.org/10.1063/1.4953234>]

I. INTRODUCTION

Recently, there is a growing interest in the study of germanium and silicon quantum dots or nanocrystals due to their efficient photoluminescence^{1–4} and the important role they play in the realization of high-performance in metal-oxide-semiconductor field-effect transistors (MOSFET).^{5,6} One of the prevailing routes for producing nanocrystals is to utilize the crystallization of amorphous films. Because grain size and crystallinity could be the important factors for achieving the desirable performances, the crystallization behavior of amorphous Si (a-Si) and Ge (a-Ge) needs to be understood. Although it is assumed that crystallization behavior depends largely on the initial amorphous structure, knowledge remains quite limited despite relatively numerous studies on the amorphous structures of Si and Ge. Investigation is therefore required on the progressive structural changes from prepared amorphous structures to crystalline phases from both the scientific and technological points of view.

For the purpose, we have examined the crystallization behavior of sputter-deposited a-Ge films induced by a low-energy electron irradiation using *in-situ* transmission electron microscopy (TEM) and by analysing the pair distribution function (PDF) from electron scattering. The combination of TEM and PDF analyses has been shown to be a powerful technique for characterizing amorphous structures.^{7,8} In

particular, since amorphous semiconductors are sensitive to electron beams,⁹ progressive structural changes towards the crystalline state can be tracked by extracting consecutive PDFs converted from the electron diffraction patterns from a particular region of a specimen under electron irradiation.¹⁰

In this paper, we report that the structural transition of a-Ge occurs due to aging at ambient temperature, which was found in the course of the investigation. In Sec. II, the differences found in the electron-induced crystallization microstructure between as-deposited and aged a-Ge are reported along with the changes in PDF of a-Ge due to aging. In Sec. III, the results of molecular dynamics (MD) simulation of a-Ge obtained by quenching liquid at different cooling rates are presented. The MD simulations were performed to understand the short- and medium-range configurations in the amorphous structure by analysing models whose average structures, represented by PDF, are similar to those experimentally observed. The origin of the unique crystallization behavior is discussed in the light of the proposed structural models such as the continuous random network (CRN) model¹¹ and the paracrystalline (PC) model,¹² on the basis of experimental and computational PDFs.

II. TEM ANALYSIS

A. Experimental procedure

Thin films of amorphous Ge, of 40 nm in thickness, were prepared by radio-frequency (RF) sputtering under a

^{a)}E-mail: nakamura@mtr.osakafu-u.ac.jp

base pressure of 3×10^{-5} Pa. The films were deposited on a cleaved rock salt crystal at an ambient temperature under 50 W of RF output power and 0.7 Pa of argon pressure. The film and the substrate were put into distilled water, and then the floating film was recovered on a molybdenum grid. The samples were aged at room temperature up to 13 months under a dry air condition.

The amorphous structures after aging at room temperature were analyzed in terms of pair distribution function (PDF). Electron-scattering patterns of the as-deposited and aged samples were obtained in the electron beam of around 300 nm in diameter and recorded on an imaging plate (Eu^{2+} -doped BaFBr). The intensity profiles were scanned by an imaging-plate processor, DITABIS Micron Vario. From the profiles, the reduced interference function, $Q i(Q)$, was calculated as a function of the magnitude of the scattering vector Q defined as $Q = 4\pi \sin \theta / \lambda$, where θ and λ are the scattering angle and the electron wavelength, respectively. Finally, a PDF was obtained from $Q i(Q)$ by the Fourier transformation.^{7,8} Electron-induced crystallization behavior of as-deposited and aged samples was also observed *in-situ* in TEM. The beam diameter was around 1.0×10^{-6} m, and the beam current was monitored with a Faraday cage. To avoid contamination, all the experiments were performed with a liquid-nitrogen cold-trap placed close to the sample holder.

B. Crystallization microstructure by electron-irradiation

The first findings that let us notice the change in the amorphous structure of a-Ge samples are the varying microstructures of electron-induced crystallization. Figure 1(a) shows a typical example of a bright-field TEM image of an as-deposited amorphous film. No effect of aging at room temperature was recognized in these images, but when these same samples were subjected to electron irradiation at high fluxes, the microstructures differed in terms of crystallization depending on the aging time. Figures 1(b)–1(e) show the bright-field images of the crystallized region by electron-irradiation in the as-deposited and aged samples. The irradiation was done at 125 keV at a high flux of $1.5 \times 10^{23} \text{ m}^{-2} \text{ s}^{-1}$ in a TEM. In the sample aged for 5 days, (b), crystalline particles of 50–100 nm grew, indicated by the dark contrast in the figures (labeled I and II). The matrix (III) consists of voids (bright spots) and the amorphous matrix. In the sample aged for 3 months, (c), crystalline particles (IV) grew and voids appeared (V), as does the case with in Fig. 1(b). However, the crystalline particles are reduced in size, and the matrix (VI) is composed of crystalline grains of around 10 nm and pores of around 3 nm in diameter. In the sample aged for longer periods of time (over 7 months), (d) and (e), only nanocrystalline grains appear along with nano-sized pores. These variations are systematic and were reproducible for twenty samples. The microstructures of Figs. 1(b) and 1(c) suggest that the atomic structure of the sputter-deposited amorphous films is inhomogeneous.

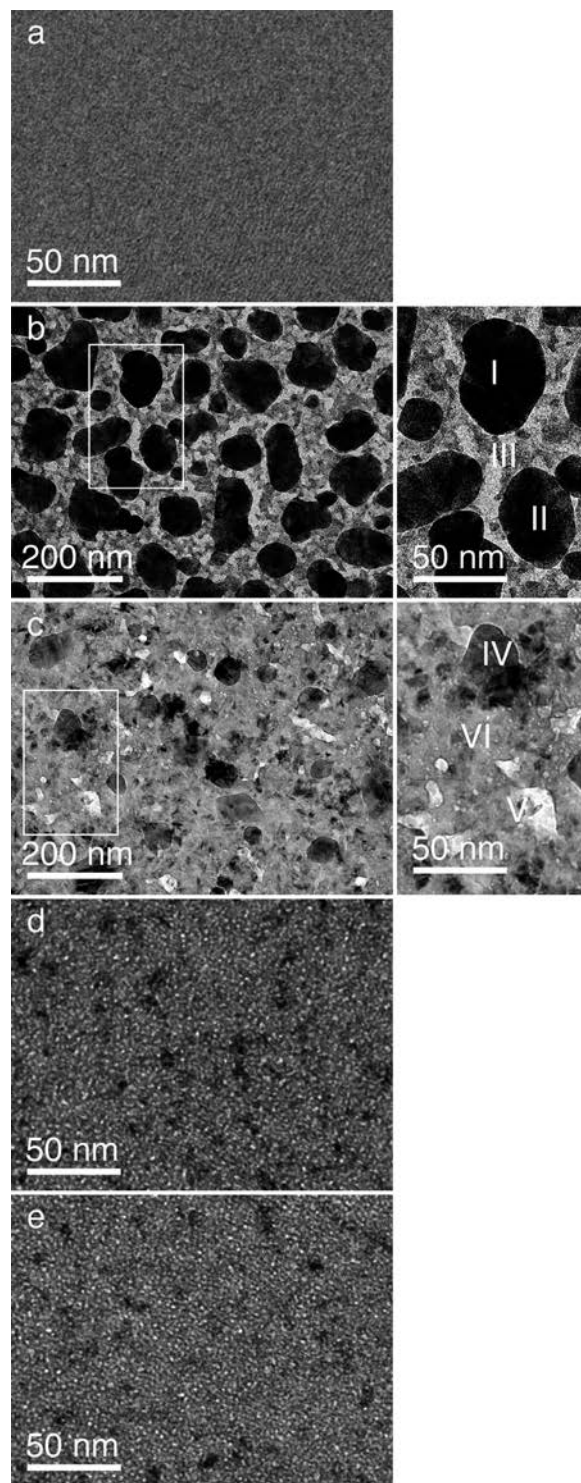


FIG. 1. Bright-field TEM images of (a) as-deposited amorphous film and (b)–(e) crystallized regions by electron irradiation. Aging time before electron irradiation: (b) 5 days, (c) 3 months, (d) 7 months, and (e) 13 months.

C. Pair distribution function

To understand the origin of these variations in the crystallized microstructures, the amorphous structures before electron irradiation were analyzed in terms of PDF. Figure 2 shows the electron scattering patterns, taken under the same exposure condition, of a-Ge films subjected to aging for (a) 3 days, (b) 3 months, (c) 7 months, and (d) 13 months at room temperature.

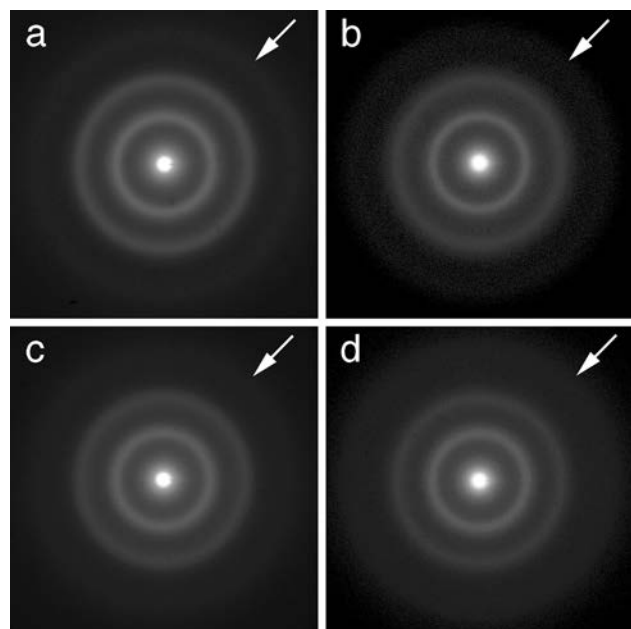


FIG. 2. Electron diffraction patterns of a-Ge samples subjected to aging at room temperature for (a) 3 days, (b) 3 months, (c) 7 months, and (d) 13 months after sample preparation. The profiles were taken under the same exposure condition. Arrows indicate third halo rings.

Slight but definite differences were noted among these patterns: the intensities of the first, second, and third (shown by arrows) halo rings are weaker and broader in the samples aged for longer time. Figure 3(a) shows the reduced interference function, $Q i(Q)$, of a-Ge films subjected to aging for 3 days, 3 months, 7 months, and 13 months at room temperature. Though the undulations of $Q i(Q)$ tend to be less accentuated for samples aged for longer time, those for the 7 and 13 months aged samples are almost identical. The PDF derived from the Fourier transform of $Q i(Q)$ exhibits the same trend, as shown in Fig. 3(b): the major peaks at around 0.245 nm, 0.398 nm, and 0.600 nm decrease in intensity and broaden with aging time up to 7 months. Another feature worthy of note is that an additional component appears at around 0.32 nm in the PDF for the samples aged for 7 and 13 months. The distance, 0.32 nm, is not close to the inter-atomic distance of Ge-O (0.24 nm¹³), Ge-H (0.16 nm¹⁴), nor Ge-N (0.183–5 nm¹⁵). This must be due not to impurities from the environment but to Ge-Ge configurations. The decrease and broadening in the major peaks and the appearance of additional atomic correlations in the PDF by aging were confirmed for ten independent samples.

III. MD SIMULATION

In order to understand the nature of the structural change which occurred with aging, details of the atomic arrangements of as-deposited and aged films are to be clarified. The MD simulations are suitable for this purpose. However, we emphasize that what we did was not to simulate the structural evolution by aging. We prepared amorphous models by cooling from the liquid state at various rates and compared the PDFs of these models with those of the previous experiment. Because the PDFs of some models were found to be

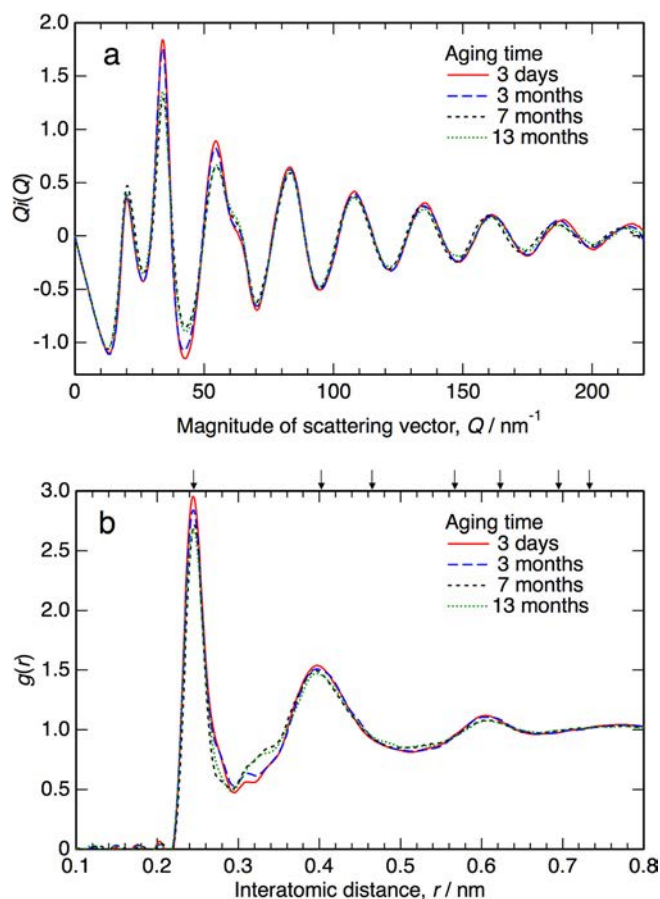


FIG. 3. (a) Reduced interference function, $Q i(Q)$, and (b) pair distribution function (PDF), $g(r)$, obtained from the electron scattering intensity profiles of a-Ge samples subjected to aging at room temperature for 3 days, 3 months, 7 months, and 13 months corresponding to the electron scattering patterns in Fig. 2. Arrows on the upper horizontal axis in (b) indicate the bond lengths in crystalline Ge with the cubic diamond structure.

almost identical to the experimental PDFs, we decided to analyze the atomic structure of these models as substitutes for the real materials.

A. Computational method

Simulations were performed by using the software package LAMMPS, a large-scale atomic/molecular massively parallel simulator.¹⁶ The Tersoff potential¹⁷ was used to represent interactions between Ge atoms with a melting temperature of 2554 K*¹⁸ (K* represents a hypothetical temperature unit in the simulation). Periodic boundary conditions were used, with a supercell of $16a_0 \times 16a_0 \times 16a_0$, where a_0 is the equilibrium lattice parameter of crystalline Ge, 0.568 nm. A total of 32 768 atoms were placed in the supercell initially at the regular positions of the diamond cubic structure. To obtain an equilibrium liquid configuration, the system was held at 4000 K* for 2 ns under the constant volume condition. Then, amorphous states were obtained by cooling the liquid from 4000 K* to 0 K* with zero external pressure. The cooling rates were set at between 4×10^{10} and 4×10^{13} K* s⁻¹. After that, the atoms were equilibrated at 633 K* for 20 ps. For the a-Ge models, the PDF and the distributions of the coordination number and the bond angle were calculated. Atoms which formed clusters

with medium-range ordered (MRO) configurations were extracted from the a-Ge matrix using the Open Visualization Tool (OVITO),¹⁹ and their concentrations were evaluated.

B. Results

Figure 4 shows computed PDFs of a-Ge models obtained by cooling the liquid at cooling rates of 4×10^{10} , 4×10^{11} , and $4 \times 10^{13} \text{ K}^* \text{ s}^{-1}$. For comparison purpose, the PDF of the liquid Ge kept at 3000 K^* is also shown. As the cooling rate increases, the intensity of the major peaks decreases and the intensity of the shoulder component at around 0.32 nm increases. This trend indicates that the amorphous structure of rapidly cooled models is close to that of a liquid model. The correlation at the shorter side of second peak is characteristic of the fifth-neighbor distances outside the first coordination shell in liquid Si.²⁰

The MRO clusters contained in the simulated a-Ge matrix are visualized by OVITO as shown in Figs. 5(a)–5(c). The MRO clusters here are defined as regions where at least five tetrahedral units are joined with two specific configurations: one is the face-centered cubic configuration characterizing the cubic diamond (in red, Fig. 5(d)), and the other is the hexagonal close-packed configuration characterizing the hexagonal diamond (in blue, Fig. 5(e)). In the slowly cooled model shown in Fig. 5(a), 11 at. % of atoms form ordered regions in the amorphous matrix. On the other hand, the concentration of atoms forming MRO clusters is at most 0.05 at. % in the amorphous structure formed by cooling at the higher rate, $4 \times 10^{13} \text{ K}^* \text{ s}^{-1}$, Fig. 5(c).

In order to characterize the differences in the amorphous structures, short-range configurations were analyzed in terms of the coordination number, N_c , and the bond angle, θ_b . Figures 6(a) and 6(b) show the distribution of N_c and θ_b , respectively, in the a-Ge models obtained with the three cooling rates and the liquid, within a distance of 0.31 nm , which corresponds to the first minimum in the PDF shown in Fig. 4. The fraction of tetrahedral units with $N_c = 4$ is dominant in the model with the lowest cooling rate, $4 \times 10^{10} \text{ K}^* \text{ s}^{-1}$. Its average coordination number is 4.05, which is almost the same as the tetrahedral diamond structure. At higher cooling

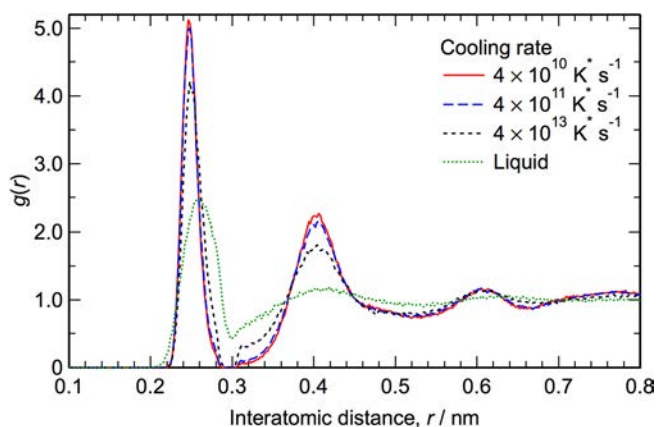


FIG. 4. PDFs of a-Ge models of the MD simulation obtained by quenching liquid Ge from 4000 K^* to 0 K^* under the different cooling rates, and by subsequent annealing at 633 K^* for 20 ps. For comparison, those for a liquid state kept at 3000 K^* are shown together.

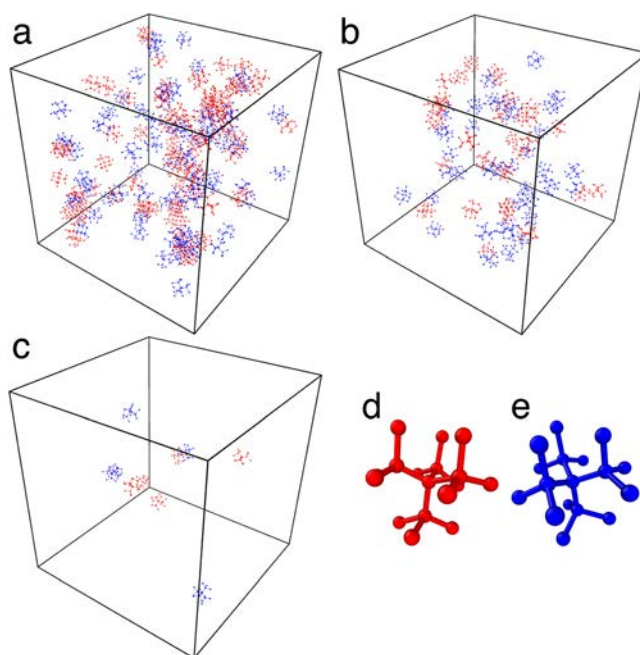


FIG. 5. Medium-range ordered (MRO) regions in a-Ge of MD simulation obtained at the cooling rates of (a) 4×10^{10} , (b) 4×10^{11} , and (c) $4 \times 10^{13} \text{ K}^* \text{ s}^{-1}$. An MRO is defined as a cluster composed of five or more tetrahedral units with two specific configurations: one is the face-centered cubic configuration characterizing the cubic diamond (in red, (d)) and the other is the hexagonal close-packed configuration characterizing the hexagonal diamond (in blue, (e)).

rates, on the other hand, the contribution of $N_c = 5$ becomes increasingly important. At $4 \times 10^{13} \text{ K}^* \text{ s}^{-1}$, in particular, atoms of $N_c = 6$ are noticeable. These features indicate that the amorphous structure obtained by more rapid cooling includes atomic configurations similar to those of a liquid model. Liquid-like features are also found in the bond angle distribution of the models produced with the high cooling rates, as shown in Fig. 6(b). In the slowly cooled model, while the bond angle is distributed symmetrically at around 109.5° , which is characteristic of the regular tetrahedral unit, the intensity is reduced, and in the rapidly cooled model, the distribution becomes asymmetric. Furthermore, additional components are recognized in the latter at around 58° and 75° : these are characteristic of over-coordinated atoms as major components of $N_c = 5$ and 6 in liquid Si²¹ and as floating bonds of $N_c = 5$ in amorphous Si.²²

IV. DISCUSSION

Electron irradiation induced the appearance of different crystallization microstructures in sputter-deposited a-Ge films: coarse and spherical nanoparticles grew rapidly in the samples aged for 3 months or less, while a homogeneous nanocrystalline structure with a grain size of about 10 nm appeared in samples aged for 7 months or longer. The experimental PDF analyses revealed that the major peaks for Ge-Ge bonds decrease in intensity and broaden with aging time up to 7 months. Furthermore, an additional component appears at around 0.32 nm in the PDF of samples aged for 7 months or longer. The MD simulations showed that the major peaks of a slowly cooled amorphous model (at

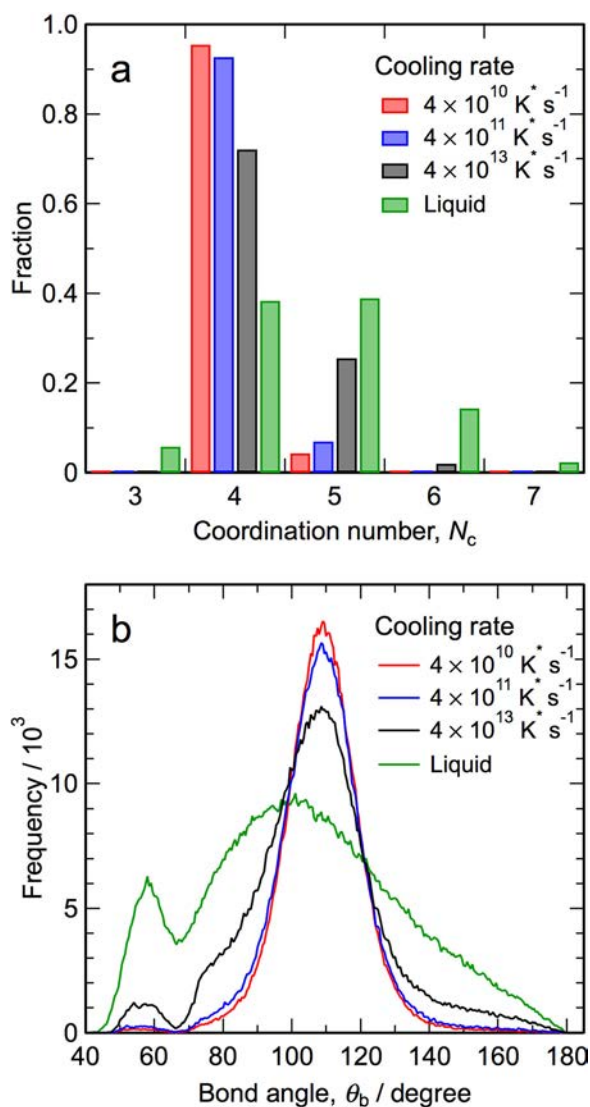


FIG. 6. (a) Distribution of the coordination number, N_c , and (b) bond-angle, θ_b , for the a-Ge models of the MD simulation of the three cooling rates. For comparison, those for a liquid state kept at 3000 K^* are also shown.

$4 \times 10^{10} \text{ K}^* \text{ s}^{-1}$) are higher in intensity and sharper than a rapidly cooled model (at $4 \times 10^{13} \text{ K}^* \text{ s}^{-1}$). The slowly cooled model includes MRO clusters composed by 11 at. % atoms. On the other hand, in the rapidly cooled model fewer than 0.1 at. % atoms compose MRO clusters, and additional atomic correlations at around 0.32 nm are common, which originate from the fifth-neighbor distance in the liquid Ge. The structural difference between the slowly cooled and rapidly cooled models is as follows: MRO clusters develop in the slowly cooled model, whereas liquid-like regions are quenched and embedded in the rapidly cooled model.

The experimental PDF analyses revealed that the amorphous structure changes toward a more random state with aging. It turned out that different crystallization microstructures reflect the change in amorphous structure. From the comparison of experimental PDFs with those of the MD models, it can be assumed that the structure of the as-deposited films and those aged for short periods of time below 3 months is similar to that of the slowly cooled MD model which includes MRO clusters, whereas the structure

of the aged films for longer periods of time over 7 months is apparently similar to that of the rapidly cooled MD model, which includes liquid-like regions but almost no MRO clusters. Furthermore, the existence of liquid-like features in fully aged films is indicated by the appearance of additional correlations at around 0.32 nm. In summary, the effect of aging can be interpreted as follows: the initial as-deposited structure contains some ordered regions embedded in a homogeneous random matrix, both with a tetrahedral configuration, and this changes with aging to a structure that contains some denser, liquid-like regions, with over-coordinated configurations in the same matrix.

Although this structural transition appears to defy common sense, transition to a less ordered structure can occur since the amorphous solids and nanoclusters embedded in them may be in a state very far from equilibrium, particularly if they were prepared by quenching from vapor rather than from liquid. The two points to be considered in the effort to understand how such a transition can occur in sputter-deposited a-Ge films are residual stress and strain energy.

Gibson and Treacy proposed the para-crystalline (PC) model for the structure of a-Si and a-Ge, in which MRO clusters are embedded in a continuous random network (CRN) matrix.¹² In this model, distorted medium-range ordered (d-MRO) clusters are considered a key component embedded in a CRN. A noteworthy characteristic of the PC model is that large strains are involved both within the d-MRO clusters themselves and also between each cluster and the CRN matrix.²³ This model seems to be applicable to vapor-deposited films, which are in an extremely non-equilibrium state. Because of the excess strain energy, the free energy of the PC structure is likely so high that the structure is unstable. Therefore, an extra strain energy, included in as-deposited a-Ge with the PC structure, may be the origin of the spontaneous structural transition to a more disordered state during room-temperature aging. Gibson and Treacy²³ reported also that thermal annealing at 350°C for 15 min reduces the degree of medium-range order in a vacuum-deposited a-Ge film. If they operate as crystalline nuclei, MRO clusters would develop directly toward crystalline grains without annihilation. Therefore, the annihilation of MRO at 350°C must be another example of the instability of initially introduced MRO clusters. The instability of MRO would be a dominant factor for both the structural transition at room temperature found in the present work and its annihilation at elevated temperature found by Gibson and Treacy, although the terminal structures by aging differ between samples kept at room temperature and those subjected to an elevated temperature (350°C). The rapid growth of coarse nanoparticles by electron irradiation into the as-deposited a-Ge samples and those aged for short period (less than 3 months), as shown in Figs. 1(b) and 1(c), may be indirect evidence that the high strain energy in the films assists the grain growth.

The bombardment of energetic particles in the deposition process of sputter-deposited thin films results in residual stress in the thin films produced:²⁴ a-Ge²⁵ and a-Si²⁶ films prepared by sputtering store compressive residual stress in the order of several GPa, for example. This is the case for the films investigated in this study, since they were prepared

by sputtering. It has been reported that thin films of a-Si and a-Ge^{27,28} and a-Ge nanoparticles with diameters below 5 nm²⁹ transform into amorphous structures of higher densities under high pressures in the order of tens of GPa. There are also a number of theoretical examples of such a transition under high pressures from a low density amorphous (LDA) form based on tetrahedral units to a high density amorphous (HDA) form with larger coordination numbers than LDA.^{30–32} The continuous random network (CRN) model,¹¹ which has been widely accepted for describing the structure of a-Si and a-Ge, is a typical LDA form. On the other hand, HDA forms involve larger coordination numbers than LDA forms and are similar to the β -Sn structure with the coordination 6 or liquid states with higher density than solids of the cubic diamond type structure.²⁹ The transition from a LDA form to a HDA form has been recognized as the nature of polyamorphism, and both a-Si and a-Ge are polyamorphic. The stress in the as-deposited films of the present study is likely high enough to induce the short-range deformation of tetrahedral units, resulting in the transition from a LDA to a HDA under high pressure, i.e., the disordering and densification of the amorphous structure.

A local amorphous-to-amorphous transition model is illustrated in Fig. 7: the as-deposited a-Ge films and those aged for short period (less than 3 months) contain some medium-range ordered regions (atoms in red) in a CRN matrix (Fig. 7(a)), whereas the films subjected to a prolonged aging period include over-coordinated atoms (in blue), which is a characteristic feature of the liquid (Fig. 7(b)), in the same matrix as (a). As shown in Fig. 7, MRO clusters (red in (a)) disintegrate and transform into liquid-like regions (blue in (b)) due to aging while maintaining the structure of the random matrix (grey in (a) and (b)).

Figure 8 illustrates schematically the structural evolution discussed above. The initial state of a-Ge films prepared by sputtering, whose structure contains distorted MRO clusters (d-MRO) in a CRN matrix, is the largest in the free energy (state I). The films aged for a long period of time changes into state II, including liquid-like regions in the same matrix. Either by heating or electron irradiation, a-Ge crystallizes into the most stable state, of the diamond structure (state V) via a homogeneous CRN structure (state III) and the development of non-distorted MRO clusters (state IV). The rapidly cooled MD models, which contain liquid-like regions in a CRN,

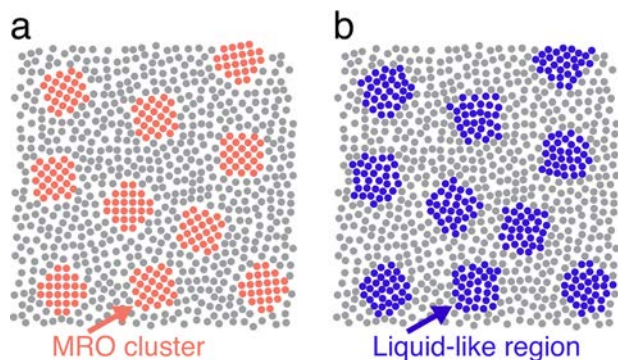


FIG. 7. A schematic illustration of structures of a-Ge (a) before and (b) after aging.

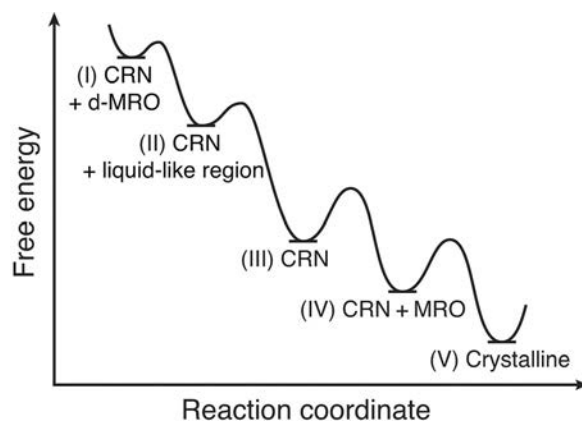


FIG. 8. A schematic free-energy diagram for structural changes of a-Ge subjected to aging and/or electron irradiation.

correspond to state II, while the slowly cooled models, in which MRO clusters develop, describe not state I but state IV. The PDF of slowly cooled models is “apparently” consistent with that of the as-deposited sample (state I), because the average structure such as short- and medium-range configurations and bond angles of state IV with non-distorted MRO clusters agrees well with that of state I with distorted MRO clusters, and an essential difference between state I and IV is probably strain. States III and IV can be induced by electron irradiation. In fact, by irradiation into the sample aged for 7 months, the intensity of the peaks in PDF recovers apparently to the level of the sample aged for 3 days (supplementary material³³), indicating that the structure changes toward crystallization, and this structure (state IV) is similar to that of the initial state, i.e., before aging (state I). Therefore, an extra strain energy, included in as-prepared a-Ge of the PC structure, may be the origin of the structural evolution during room-temperature aging.

V. SUMMARY

The structural transition in amorphous Ge films prepared by sputter-deposition under aging at ambient temperature was studied by means of PDF by TEM. The molecular dynamics simulations were performed to discern the atomic structure of the as-deposited and aged-films, by analyzing detailed atomic arrangements in amorphous models with similar average structure (PDFs) to those in the experiment. The results and conclusions are summarized as follows:

- (1) In the pair distribution functions of the as-deposited and aged samples, the major peaks for Ge-Ge bonds decreased in intensity and broadened with aging up to 7 months and longer. The results indicate that the structure becomes a more random/disordered state due to aging. In particular, the existence of liquid-like features in fully aged films is indicated by the appearance of additional correlations at around 0.32 nm.
- (2) The MD simulations show that the major peaks in the PDF are higher in intensity and sharper in a slowly cooled model (at $4 \times 10^{10} \text{ K}^* \text{ s}^{-1}$) than in a rapidly cooled model (at $4 \times 10^{13} \text{ K}^* \text{ s}^{-1}$). In the slowly cooled model, 11 at. % atoms formed MRO clusters. On the

other hand, the rapidly cooled model was characterized by liquid-like configurations rather than MRO clusters.

- (3) A comparison of the experimental PDFs to those of MD models suggests the difference in structure between the as-deposited sample and the aged samples for short periods of time around 3 months, and the samples aged for longer than 7 months. The structure of the former can be described by that of the slowly cooled MD model characterized by MRO clusters, whereas the structure of the latter includes liquid-like regions but no MRO clusters like the rapidly cooled MD model. The similarities between the PDFs of the real films and MD models suggest that the initially as-deposited structure, which includes some ordered regions, becomes more random/disordered with liquid-like regions. The local transition from MRO clusters to liquid-like regions due to aging at room temperature likely originates from the existence of unstable MRO clusters under an extreme non-equilibrium state introduced by the vapor-deposition process.

ACKNOWLEDGMENTS

TEM observations were supported by Osaka University Microstructural Characterization Platform as a program “Nanotechnology Platform” of the Ministry of Education, Culture, Sports, Science and Technology (MEXT), Japan. We are grateful to Dr. T. Sakata and Dr. T. Nagase, and Mr. E. Taguchi for their technical support with TEM operations. We appreciate Dr. T. Ichitsubo of Kyoto University for fruitful discussion. This work was supported by Grant-in-Aid for Scientific Research (C) of MEXT, No. 26420727.

- ¹S. Takeoka, M. Fujii, S. Hayashi, and K. Yamamoto, *Phys. Rev. B* **58**, 7921 (1998).
²Y. M. Niquet, G. Allan, C. Delerue, and M. Lannoo, *Appl. Phys. Lett.* **77**, 1182 (2000).
³H. C. Weissker, J. Furthmüller, and F. Bechstedt, *Phys. Rev. B* **65**, 155328 (2002).
⁴S. J. Jensen, L. T. P. Pedersen, R. Pereira, J. Chevallier, L. J. Hansen, B. B. Nielsen, and N. A. Larsen, *Appl. Phys. A* **83**, 41 (2006).

- ⁵C. O. Chui, L. Kulig, J. Moran, W. Tsai, and K. C. Saraswat, *Appl. Phys. Lett.* **87**, 091909 (2005).
⁶K. Usuda, Y. Kamata, Y. Kamimuta, T. Mori, M. Koike, and T. Tezuka, *Appl. Phys. Exp.* **7**, 056501 (2014).
⁷T. Ohkubo and Y. Hirotsu, *Phys. Rev. B* **67**, 094201 (2003).
⁸M. Ishimaru, *Nucl. Instrum. Methods Phys. Res., Sect. B* **250**, 309 (2006).
⁹I. Jenčič, M. W. Bench, I. M. Robertson, and M. A. Kirk, *J. Appl. Phys.* **78**, 974 (1995).
¹⁰R. Nakamura, M. Ishimaru, H. Yasuda, and H. Nakajima, *J. Appl. Phys.* **113**, 064312 (2013).
¹¹D. E. Polk, *J. Non-Cryst. Solids* **5**, 365 (1971).
¹²M. M. J. Treacy and K. B. Borisenko, *Science* **335**, 950 (2012).
¹³J. Peralta, G. Gutiérrez, and J. Rogan, *J. Phys. Condens. Matter* **20**, 145215 (2008).
¹⁴P. K. Sitch, T. Frauenheim, and R. Jones, *J. Phys. Condens. Matter* **8**, 6873 (1996).
¹⁵C. L. Bull, P. F. McMillan, J.-P. Itié, and A. Polian, *Phys. Status Solidi A* **201**, 909 (2004).
¹⁶S. Plimpton, *J. Comput. Phys.* **117**, 1 (1995).
¹⁷J. Tersoff, *Phys. Rev. B* **39**, 5566 (1989).
¹⁸J. S. Cook and P. Clancy, *Phys. Rev. B* **47**, 7686 (1993).
¹⁹A. Stukowski, *Modell. Simul. Mater. Sci. Eng.* **18**, 015012 (2010).
²⁰S. Sastry and C. A. Angell, *Nat. Mater.* **2**, 739 (2003).
²¹C. Liu, Z. Zhu, J. Xia, and D. Sun, *Phys. Rev. B* **60**, 3194 (1999).
²²M. Ishimaru, *J. Phys. Condens. Matter* **13**, 4181 (2001).
²³J. M. Gibson and M. M. J. Treacy, *Phys. Rev. Lett.* **78**, 1074 (1997).
²⁴H. Windischmann, *J. Appl. Phys.* **62**, 1800 (1987).
²⁵T. Zhan, Y. Xu, M. Goto, Y. Tanaka, R. Kato, M. Sasaki, and Y. Kagawa, *AIP Adv.* **4**, 027126 (2014).
²⁶J. D. Mugiraneza, T. Miyahira, A. Sakamoto, Y. Chen, T. Okada, T. Noguchi, and T. Itoh, *Jpn. J. Appl. Phys., Part 1* **49**, 121302 (2010).
²⁷O. Shimomura, S. Minomura, N. Sakai, K. Asaumi, K. Tamura, J. Fukushima, and H. Endo, *Philos. Mag.* **29**, 547 (1974).
²⁸E. Principi, A. Di Cicco, F. Decremps, A. Polian, S. De Panfilis, and A. Filippini, *Phys. Rev. B* **69**, 201201 (2004).
²⁹N. R. C. Corsini, Y. Zhang, W. R. Little, A. Karatutlu, O. Ersoy, P. D. Haynes, C. Molteni, N. D. M. Hine, I. Hernandez, J. Gonzalez, F. Rodriguez, V. V. Brazhkin, and A. Sapelkin, *Nano Lett.* **15**, 7334 (2015).
³⁰J. Kōga, F. Yonezawa, K. Nishio, and T. Yamaguchi, *J. Non-Cryst. Solids* **345–346**, 742 (2004).
³¹P. F. McMillan, M. Wilson, D. Daisenberger, and D. Machon, *Nat. Mater.* **4**, 680 (2005).
³²O. I. Barkalov, V. G. Tissen, P. F. McMillan, M. Wilson, A. Sella, and M. V. Nefedova, *Phys. Rev. B* **82**, 020507 (2010).
³³See supplementary material at <http://dx.doi.org/10.1063/1.4953234> for the PDF of a sample aged for 7 months (broken black) and that of the same sample after irradiation of electrons at a flux of $6.9 \times 10^{22} \text{ m}^{-2} \text{ s}^{-1}$ for 60 min (dashed blue). The PDF for a sample aged for 3 days (solid red) is shown together for comparison.